03,09

Creating NV^--defects in silicon carbide $6H$-SiC by irradiation with high-energy electrons

© F.F. Murzakhanov[1], Yu.A. Uspenskaya[2,¶], E.N. Mokhov[2], O.P. Kazarova[2], V.V. Kozlovski[3], V.A. Soltamov[2]

[1] Institute of Physics, Kazan Federal University,
Kazan, Russia
[2] Ioffe Institute,
St. Petersburg, Russia
[3] Peter the Great Saint-Petersburg Polytechnic University,
St. Petersburg, Russia

¶ E-mail: yulia.uspenskaya@mail.ioffe.ru

Received February 26, 2024
Revised February 26, 2024
Accepted February 27, 2024

The possibility of creating negatively charged nitrogen-vacancy defects (NV^-) in crystals of hexagonal ($6H$) silicon carbide by irradiating the latter with high-energy electrons ($E = 2$ MeV) and subsequent high-temperature annealing at $T = 900°C$ was investigated. Using electron paramagnetic resonance (EPR) it was shown that SiC crystals contain triplet ($S = 1$) centers of axial symmetry with fine structure parameters $D = 1344$, 1318 and 1268 MHz. The corresponding components of the fine structure are split by a spectrally resolved hyperfine interaction with the nuclear spin of nitrogen (^{14}N, $I = 1$), which is characterized by a hyperfine interaction constant $A \approx 1.23$ MHz, which makes it possible to unambiguously identify the presence of NV^--centers in the samples under study. It is shown that optical excitation by an IR laser $\lambda = 980$ nm leads to the creation of an inverse population of the spin sublevels of these triplet centers, which is the basis for their use as quantum sensors, qubits and masers with optical pumping.

Keywords: electron paramagnetic resonance, silicon carbide, nitrogen-vacancy defect.

DOI: 10.61011/PSS.2024.04.58194.35

1. Introduction

Defects with a high spin ground state ($S \geq 1$) in crystal matrices with a wide band gap play an important role in the development of quantum technologies [1–5]. The spin sublevels of such defects can be initialized, controlled and read using optical or radio frequency methods, providing access to spin control [1–5]. A negatively charged nitrogen vacancy center in diamond (NV^-) is a vivid example of such a defect. Quantum sensors of magnetic fields, temperature and pressure, masers operating at room temperature were developed using the spin and optical properties of diamond NV^--centers [4,6,7]. Currently, an active search is underway for similar defects in materials that are more technologically suitable than diamonds [1,2,8]. The most notable results in this direction have been achieved on a semiconductor material with developed technologies produced on a commercial scale, namely silicon carbide (SiC) [1,8,9]. In particular, triplet ($S = 1$) and quadruplet ($S = 3/2$) defects with the property of optically induced inverse occupancy of spin sublevels in the ground state, spin-dependent fluorescence, allowing the registration of an optically detectable magnetic resonance signal, were discovered and identified [1,8,9]. It should be noted that active studies of such defects are conducted in all major SiC polytypes ($4H$, $6H$, $3C$, $15R$) [9–11].

Another triplet center has been recently added to these families of defects in SiC, namely, a negatively charged nitrogen vacancy defect, which is a negatively charged silicon vacancy (V_{Si}^-) and the nitrogen atom closest to it in the carbon atom substitution position (N_C) — $N_C V_{Si}$ [12,13]. The structure of the defect in hexagonal silicon carbide of the polytype $6H$ is shown in Figure 1, *a*. It should be noted that the polytype $6H$ is characterized by three unequal positions in the lattice including one hexagonal (h) and two quasi-cubic ($k1, k2$). Thus, the paired $N_C V_{Si}$-defect in $6H$ can be formed in the form of three axial configurations NV_{hh}, NV_{k2k1} and NV_{k1k2} and three basal NV_{hk1}, NV_{k1h}, NV_{k2k2}. Only axial configurations will be considered in this paper. The unique conformance of the structure of this defect to the structure of the NV-center in diamond, shown earlier [14,15], the presence of a spin-dependent infrared photoluminescence channel (NIR PL) and an intercombination conversion channel (Figure 1, *b*), resulting in the inverse population in the ground state open wide prospects for using NV-defects in a more technologically advanced platform compared to diamond, such as SiC. It should be noted that the properties of NV-defects in SiC are currently studied in all available polytypes, and an active study of methods for their generation is underway. In particular, it was shown that these defects can be created by irradiation of SiC crystals with protons or ions (N, Si, I) and subsequent annealing at temperatures of 900−1000°C [12,16]. The

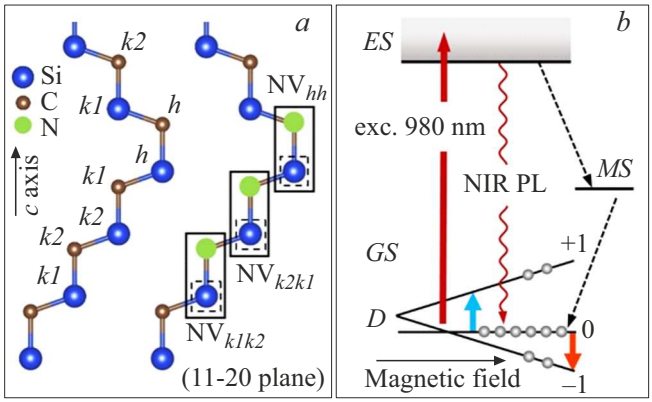

Figure 1. (*a*) View of the lattice 6*H*-SiC in the plane (11−20). Hexagonal (*h*) and quasi-cubic (*k1, k2*) non-equivalent positions are indicated respectively. Silicon vacancies are shown by dotted lines, and paired NV-defects are marked by rectangles. (*b*) The energy structure of the optical pumping cycle of the spin sublevel $m_s = 0$ of the main (*GS*) triplet state of $S = 1$ NV-centers. The dotted arrows show spin-dependent recombination from the excited state (*ES*) to *GS* through the metastable state (*MS*) under the action of optical excitation ($\lambda = 980$ nm). Spin-dependent luminescence is designated as NIR PL. The separation of spin sublevels in the absence of a magnetic field is indicated by the fine structure parameter *D*. The external magnetic field causes the Zeeman splitting of the ground state. The vertical arrows show the allowed EPR transitions between the spin sublevels of the triplet.

applicability of ion implantation of nitrogen in ultrapure epitaxial layers of SiC was demonstrated for creating single NV-defects [17].

Unlike proton and ion irradiation, electron irradiation is the best method for the homogeneous introduction of vacancy defects, which allows for creation of defects, avoiding their clustering. This circumstance is well documented by the example of studies of the properties of NV-defects in diamond. In particular, the appropriate choice of electron energy, radiation dose and annealing parameters allow obtaining diamond samples with an optimal concentration of NV-defects, which are used as references for quantum magnetometry using ensembles of defects in diamond [18,19]. Tools of reproducible and controlled formation of NV-defects in the crystal structure are necessary for studying and improving the characteristics of NV-defects in silicon carbide.

We demonstrate in this study that the irradiation of SiC with electrons with an energy of 2 MeV and subsequent high-temperature annealing is such a tool.

2. Experimental part

Crystals of silicon carbide 6*H*-^{28}SiC with a reduced content of the magnetic isotope ^{29}Si ($I = 1/2$) were grown by high-temperature physical vapor transport (PVT) using a precursor enriched with the isotope ^{28}Si [20]. A substrate of 6*H*-SiC with a natural content of isotopes ^{29}Si (natural abundance 4.7%) and ^{13}C ($I = 1/2$, natural abundance 1.1%) was used as a seed. Concentration of the isotope ^{28}Si in grown samples by the EPR method, revealed the content of this isotope at the level of 99%, which corresponds to a four-fold reduction of the content of ^{29}Si [21]. The concentration of nitrogen atoms in the grown samples was $N_d \approx 10^{17}$ cm^{-3}. The grown samples were irradiated with electrons with an energy of $E = 2$ MeV and a dose of $4 \cdot 10^{18}$ cm^{-2} for creation of vacancy defects. The irradiated crystals were annealed at a temperature of $T = 900$°C in an argon atmosphere for 2 h. EPR studies of samples were conducted using commercial EPR spectrometer Bruker Elexsys 680 in the X-range (≈ 9.73 GHz).

3. Results and discussion

The EPR spectrum of the irradiated and annealed sample of 6*H*-^{28}SiC is shown in Figure 2. The spectrum was recorded with an optical excitation by a 980 nm laser with a parallel orientation of the permanent magnetic field of the hexagonal crystallographic axis ***c*** of the crystal 6*H* ($\boldsymbol{B} \parallel \boldsymbol{c}$). It can be seen that the spectrum contains three doublets of lines, indicated in Figure 2 as NV$_{hh}$, NV$_{k2k1}$ and NV$_{k1k2}$. The lines are arranged symmetrically relative to the magnetic field $\boldsymbol{B}_0$ corresponding to $g = 2.00$. The structure of the spectrum reflects the presence of splitting in the zero magnetic field *D* between the spin sublevels of triplet defects caused mainly by spin-spin interaction. The spectrum can be described by a spin Hamiltonian of axial symmetry of the form (1), including the Zeeman interaction and a term describing the splitting of spin sublevels in a zero magnetic field, the presence of which results in the occurrence of a fine structure in the EPR spectrum:

$$H = g\mu_B \boldsymbol{B} \cdot \boldsymbol{S} + D(S_z^2 - 2/3), \qquad (1)$$

where $\boldsymbol{S}$ — the electron spin operator, $g\mu_B = 2.8$ MHz/G — the gyromagnetic ratio for an electron, g — the spectroscopic splitting factor, $\boldsymbol{B}$ — the constant magnetic field, *D* — the fine structure parameter (zero splitting), S_z — the spin projection operator of the triplet center. In accordance with the spin Hamiltonian, the resonant magnetic fields of each pair of lines are characterized by splitting $\Delta B = 2D/g\mu_B$ and correspond to the permitted EPR transitions $\Delta m_s = \pm 1$. For a pair of lines designated as NV$_{k2k1}$, the value of $\Delta B = 906$ G, for NV$_{hh}$ and NV$_{k1k2}$, this value is 942 and 960 G, respectively. Thus, the parameter *D*, determined using the EPR spectrum for each triplet center, has the following values: D (NV$_{k2k1}$) = 1268 MHz, D (NV$_{hh}$) = 1318 MHz, D (NV$_{k1k2}$) = 1344 MHz. These values of the parameter *D*, which constitute an unambiguous spectroscopic feature for identifying the paramagnetic center, are in good agreement with previously defined parameters, namely D (NV$_{k2k1}$) = 1278 MHz, D (NV$_{hh}$) = 1328 MHz, D (NV$_{k1k2}$) = 1355 MHz [12].

A slight deviation of the values previously established in [12] from the values given by us can be explained by the temperature dependence of the parameter of the fine structure of NV-centers observed for the case of NV-centers both in diamond [22] and in SiC [23], taking into account that the data in [12] were obtained with low-temperature measurements ($T = 10$ K) of EPR spectra. A detailed study of the structure of spectral lines was conducted for observing the splitting caused by the hyperfine interaction (HFI) of the electron spin of the NV-center with the nuclear spin of the nitrogen atom included in the structure of the center for more reliable identification of NV-defects in the samples. The HFI is described by an additional member of the form $\boldsymbol{S} \cdot \boldsymbol{A} \cdot \boldsymbol{I}$ to the spin Hamiltonian (1). Here $\boldsymbol{A}$ is the hyperfine interaction tensor, $\boldsymbol{I}$ is the nuclear spin operator ($I = 1$ for ^{14}N). It was previously shown that the magnitude of the hyperfine interaction for NV-centers in SiC does not exceed 1.5 MHz and is practically isotropic (anisotropy does not exceed 200 kHz) [12,14,15]. Figure 3 shows the EPR lines of NV_{hh}, NV_{k2k1} and NV_{k1k2} centers recorded in the X-band, with a small amplitude of magnetic field modulation 0.1 G. The VHF power was selected as the minimum ($P = 60$ dB). Nevertheless, it can be seen that saturation of the EPR lines of NV-defects occurs even at minimum power because of long spin-lattice relaxation times (T_1). It is apparent that each line is split into three

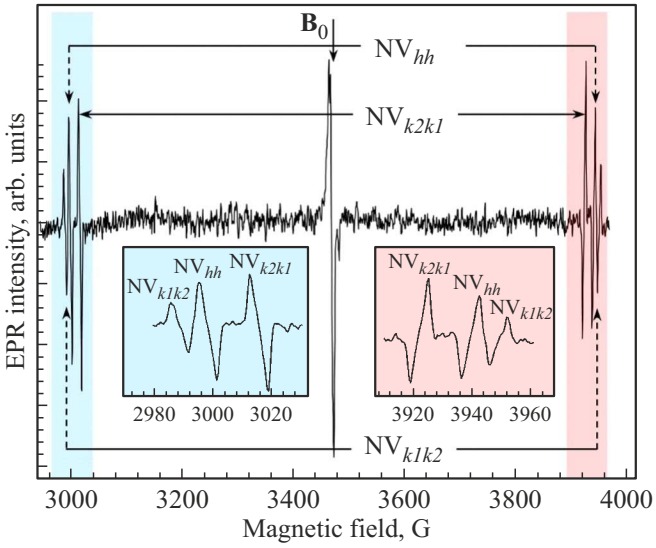

Figure 2. The EPR spectrum of the sample of 6*H*-^{28}SiC irradiated with electrons and annealed at 900°C, recorded with magnetic field modulation 5 G, temperature $T = 150$ K and laser excitation $\lambda = 980$ nm. The orientation of the magnetic field $\boldsymbol{B} \parallel \boldsymbol{c}$. The resonant magnetic fields corresponding to the permitted transitions between the spin sublevels of triplet centers, shown in the inserts on an enlarged scale, are designated as NV_{hh}, NV_{k2k1} and NV_{k1k2}. The colors show the enhanced absorption and radiation of microwaves, in accordance with the diagram of triplet sublevels in Figure 1. The magnetic field $\boldsymbol{B}_0$, corresponding to the center of mass of the triplet spectra (g-factor $g = 2.00$), is shown by a vertical arrow.

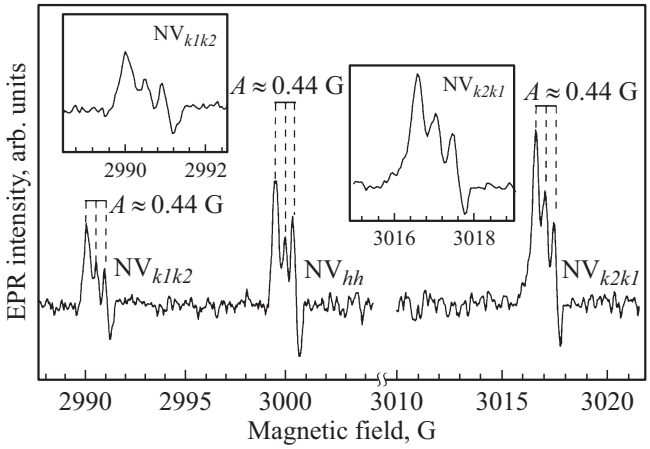

Figure 3. Components of the fine structure NV_{hh}, NV_{k2k1} and NV_{k1k2} corresponding to magnetic dipole transitions between spin sublevels $m_s = 0 \leftrightarrow m_s = +1$ were recorded with a magnetic field modulation of 0.1G, temperature $T = 150$ K and laser excitation $\lambda = 980$ nm. The orientations of magnetic field $\boldsymbol{B} \parallel \boldsymbol{c}$. The hyperfine structure of each component, consisting of three lines, is shown by vertical dash lines. The constant of HFI with nuclear spin ^{14}N for each center is denoted as A and is equal to ≈ 0.44 G. The inserts show the signals of NV_{k2k1} and NV_{k1k2} at an enlarged scale for a better illustration of HFI.

equidistant components characterized by the magnitude of the hyperfine interaction $A \approx 0.44$ G (1.23 MHz).

The number of lines of an hyperfine structure

$$N = 2n \cdot I + 1 = 3,$$

where n corresponds to the number of equivalent nuclei ($n = 1$ for the NV-center), and $I = 1$ — the value of the nuclear spin ^{14}N, and the value of the HFI is of the order 1.23 MHz, uniquely identify defects as NV_{hh}, NV_{k2k1} and NV_{k1k2}.

4. Conclusion

The possibility of radiation doping of silicon carbide for creation of quantum sensors and qubits is considered this paper. The study of radiation defects in SiC in most cases is related to the issues of radiation resistance of devices on its base. The consistency of electron irradiation and high-temperature annealing for creating NV-centers in silicon carbide of the polytype 6*H* with a modified isotopic composition is shown by the electron paramagnetic resonance method. The combination of EPR data on the values of the spectroscopic parameters of the fine structure of D and the values of the hyperfine interaction of $A \approx 0.44$ G (1.23 MHz) with nitrogen unambiguously suggest the presence of NV-defects in the studied sample of 6*H*-^{28}SiC. This method of creation of NV-centers is a reference method for generation of NV-centers in diamond, especially for creation of quantum sensors characterized by a uniform distribution of defects over the sample

volume [18,19]. It should also be emphasized that triplet centers in 6*H*-SiC were previously observed, which also showed the presence of HFI with nuclear spin ^{14}N [24,25]. However, the values of the parameter D (3.4 GHz [24], 2.6 GHz [25]) and the parameter A ($\approx$ 5 G [24,25]) greatly differ in these papers from the values given in this paper and obtained earlier in Ref. [12]. Thus, the centers considered in this paper are different from those identified in Ref. [24,25]. A unique opportunity opens up to transfer the techniques and methods of using NV-centers previously developed on the diamond platform to NV-centers in SiC since silicon carbide is a high-tech semiconductor material, and NV-centers in it are a direct substitute of NV-centers in a diamond. This feature has been intensively implemented recently [17,26,27]. A distinctive feature of the results presented in the paper is the use of isotopically pure silicon carbide, practically devoid of nuclear magnetic moments associated with ^{29}Si, which opens up broad opportunities for studying the coherent properties of NV-centers in isotopically pure samples [28]. The latter is of particular interest in light of the demonstration of ultrahigh coherence times of NV-centers in isotopically pure diamonds (enriched with the isotope ^{12}C) [29] and opens up additional opportunities for using NV-centers as qubits.

Funding

The study was supported by a grant from the Russian Science Foundation No. 22-12-00003, https://rscf.ru/project/22-12-00003/.

Conflict of interest

The authors declare that they have no conflict of interest.

References

[1] D. Awschalom, R. Hanson, J. Wrachtrup, B.B. Zhou. Nature Photon. **12**, 516 (2018).
[2] P.G. Baranov, H.J. von Bardeleben, F. Jelezko, J. Wrachtrup. Springer Ser. Mater. Sci. **253**, 448 (2017).
[3] D. Suter. Magn. Res. **1**, 115 (2020).
[4] M.W. Doherty, N.B. Manson, P. Delaney, F. Jelezko, J. Wrachtrup, L.C.L. Hollenberg. Phys. Rep. **528**, 1 (2013).
[5] A. Gottscholl, M. Kianinia, V. Soltamov, S. Orlinskii, G. Mamin, C. Bradac, C. Kasper, K. Krambrock, A. Sperlich, M. Toth, I. Aharonovich, V. Dyakonov. Nature Mater **19**, 540 (2020).
[6] N. Aslam, M. Pfender, P. Neumann, R. Reuter, A. Zappe, F.F. de Oliveira, A. Denisenko, H. Sumiya, Sh. Onoda, J. Isoya, J. Wrachtrup. Science **357**, *6346*, 67 (2017).
[7] J.D. Breeze, E. Salvadori, J. Sathian, N.McN. Alford, Ch.W.M. Kay. Nature **555**, 493 (2018).
[8] S.A. Tarasenko, A.V. Poshakinskiy, D. Simin, V.A. Soltamov, E.N. Mokhov, P.G. Baranov, V. Dyakonov, G.V. Astakhov. Phys. Status Solidi B **255**, 1700258 (2018).
[9] G.V. Astakhov, D. Simin, V. Dyakonov, B.V. Yavkin, S.B. Orlinskii, I.I. Proskuryakov, A.N. Anisimov, V.A. Soltamov, P.G. Baranov. Appl. Magn. Res. **47**, 793 (2016).
[10] A.L. Falk, B.B. Buckley, G. Calusine, W.F. Koehl, V.V. Dobrovitski, A. Politi, C.A. Zorman, P.X.-L. Feng, D.D. Awschalom. Nature Commun. **4**, 1819 (2013).
[11] T. Biktagirov, W. Gero Schmidt, U. Gerstmann, B. Yavkin, S. Orlinskii, P. Baranov, V. Dyakonov, V. Soltamov. Phys. Rev. B **98**, 195204 (2018).
[12] A. Csóré, H.J. von Bardeleben, J.L. Cantin, A. Gali. Phys. Rev. B **96**, 085204 (2017).
[13] Kh. Khazen, H.J. von Bardeleben, S.A. Zargaleh, J.L. Cantin,1 Mu Zhao, W. Gao, T. Biktagirov, U. Gerstmann. Phys. Rev. B **100**, 205202 (2019).
[14] F.F. Murzakhanov, B.V. Yavkin, G.V. Mamin, S.B. Orlinskii, H.J. von Bardeleben, T. Biktagirov, U. Gerstmann, V.A. Soltamov. Phys. Rev. B **103**, 245203 (2021).
[15] F.F. Murzakhanov, M.A. Sadovnikova, G.V. Mamin, S.S. Nagalyuk, H.J. von Bardeleben, W.G. Schmidt, T. Biktagirov, U. Gerstmann, V.A. Soltamov. J. Appl. Phys. **134**, 123906 (2023).
[16] S.I. Sato, T. Narahara, Y. Abe, Y. Hijikata, T. Umeda, T. Ohshima. J. Appl. Phys. **126**, 083105 (2019).
[17] J.-F. Wang, F.-F. Yan, Q. Li, Z.-H. Liu, H. Liu, G.-P. Guo, L.-P. Guo, X. Zhou, J.-M. Cui, J. Wang, Z.-Q. Zhou, X.-Y. Xu, J.-S. Xu, C.-F. Li, G.-C. Guo. Phys. Rev. Lett. **124**, 223601 (2020).
[18] V.M. Acosta, E. Bauch, M. P. Ledbetter, C. Santori, K.-M.C. Fu, P.E. Barclay, R.G. Beausoleil, H. Linget, J.F. Roch, F. Treussart, S. Chemerisov, W. Gawlik, D. Budker. Phys. Rev. B **80**, 115202 (2009).
[19] T. Wolf, P. Neumann, K. Nakamura, H. Sumiya, T. Ohshima, J. Isoya, J. Wrachtrup. Phys. Rev. X **5**, 041001 (2015).
[20] Yu.A. Vodakov, E.N. Mokhov, M.G. Ramm, A.D. Roenkov. Krist. Tech. **14**, 729 (1979).
[21] V.A. Soltamov, C. Kasper, A.V. Poshakinskiy, A.N. Anisimov, E.N. Mokhov, A. Sperlich, S.A. Tarasenko, P.G. Baranov, G.V. Astakhov, V. Dyakonov. Nature Commun. **10**, 1678 (2019).
[22] R.A. Babunts, A.A. Soltamova, D.O. Tolmachev, V.A. Soltamov, A.S. Gurin, A.N. Anisimov, V.L. Preobrazhenskii, P.G. Baranov. JETP Lett. **95**, *8*, 429 (2012).
[23] H.J. von Bardeleben, J.L. Cantin, E. Rauls, U. Gerstmann. Phys. Rev. B **92**, 064104 (2015).
[24] N. Bagraev, E. Danilovskii, D. Gets, E. Kalabukhova, L. Klyachkin, A. Malyarenko, D. Savchenko, B. Shanina. AIP Conf. Proc. **1583**, 243 (2014).
[25] M.V. Muzafarova, I.V. Ilyin, E.N. Mokhov, V.I. Sankin, P.G. Baranov. Mater. Sci. Forum **527–529**, Part *1*, 555 (2006).
[26] Zh. Jiang, H. Cai, R. Cernansky, X. Liu, W. Gao. Sci. Adv. **9**, eadg2080 (2023).
[27] F. Murzakhanov, M. Sadovnikova, G. Mamin, K. Sannikov, A. Shakirov, H.J. von Bardeleben, E. Mokhov, S. Nagalyuk. Appl. Phys. Lett. **124**, 034001 (2024).
[28] V.A. Soltamov, B.V. Yavkin, A.N. Anisimov, H. Singh, A.P. Bundakova, G.V. Mamin, S.B. Orlinskii, E.N. Mokhov, D. Suter, P.G. Baranov. Phys. Rev. B **103**, 195201 (2021).
[29] E.D. Herbschleb, H. Kato, Y. Maruyama, T. Danjo, T. Makino, S. Yamasaki, I. Ohki, K. Hayashi, H. Morishita, M. Fujiwara, N. Mizuochi. Nature Commun. **10**, 3766 (2019).

Translated by A.Akhtyamov